Gamow-Teller transitions in the $A = 40$ isoquintet of relevance for neutrino captures in ^{40}Ar

M. Karakoç,[1,2] R. G. T. Zegers,[3,4,5,*] B. A. Brown,[3,4,5] Y. Fujita,[6,7] T. Adachi,[6] I. Boztosun,[1,2] H. Fujita,[6] M. Csatlós,[8] J. M. Deaven,[3,4,5,†] C. J. Guess,[3,4,5,‡] J. Gulyás,[8] K. Hatanaka,[6] K. Hirota,[6] D. Ishikawa,[6] A. Krasznahorkay,[8] H. Matsubara,[6,§] R. Meharchand,[3,4,5,‖] F. Molina,[9,¶] H. Okamura,[6,**] H. J. Ong,[6] G. Perdikakis,[3,4,5,††] C. Scholl,[10,‡‡] Y. Shimbara,[11,§§] G. Susoy,[12] T. Suzuki,[6] A. Tamii,[6] J. H. Thies,[13] and J. Zenihiro[6,‖‖]

[1]*Department of Physics, Akdeniz University, 07058 Antalya, Turkey*
[2]*Nuclear Science Application and Research Center, Akdeniz University, 07058 Antalya, Turkey*
[3]*National Superconducting Cyclotron Laboratory, Michigan State University, East Lansing, Michigan 48824-1321, USA*
[4]*Joint Institute for Nuclear Astrophysics, Michigan State University, East Lansing, Michigan 48824, USA*
[5]*Department of Physics and Astronomy, Michigan State University, East Lansing, Michigan 48824, USA*
[6]*Research Center for Nuclear Physics, Osaka University, Ibaraki, Osaka 567-0047, Japan*
[7]*Department of Physics, Osaka University, Toyonaka, Osaka 560-0043, Japan*
[8]*Institute for Nuclear Research (MTA-Atomki), Post Office Box 51, H-4001 Debrecen, Hungary*
[9]*Instituto de Física Corpuscular, CSIC-Universidad de Valencia, E-46071 Valencia, Spain*
[10]*Institut für Kernphysik, Universität zu Köln, D-50937 Köln, Germany*
[11]*Graduate School of Science and Technology, Niigata University, Nishi, Niigata 950-2181, Japan*
[12]*Department of Physics, Istanbul University, Istanbul 34134, Turkey*
[13]*Institut für Kernphysik, Westfälische Wilhelms-Universität, D-48149 Münster, Germany*

(Received 26 January 2014; revised manuscript received 18 May 2014; published 24 June 2014)

Background: The Gamow-Teller response of ^{40}Ar is important for the use of liquid argon as a medium for neutrino detection. An ambiguity about the Gamow-Teller strength for the excitation of 1^+ states at 2290 and 2730 keV in ^{40}K results in a significant uncertainty for neutrino capture rates. This ambiguity is caused by the large discrepancy observed between strengths extracted from ^{40}Ar(p,n) charge-exchange data and the transition strengths for the analog transitions studied in the β decay of ^{40}Ti.

Purpose: This study was aimed at resolving the ambiguity between the results from the ^{40}Ar(p,n) charge-exchange and ^{40}Ti β-decay data.

Method: Shell-model calculations in the sd-pf shell with a new interaction (WBMB-C) were used to study differences between the structure of the transitions from ^{40}Ar and ^{40}Ti. Distorted-wave Born approximation reaction calculations were used to investigate uncertainties in the extraction of Gamow-Teller strength from the ^{40}Ar(p,n) data. New high-resolution data for the ^{40}Ar(^{3}He,t) reaction were used to gain further insight into the charge-exchange reaction mechanism and to provide more information to test the validity of the shell-model calculations.

Results: The shell-model calculations showed that interference between amplitudes associated with pf and sd components to the low-lying Gamow-Teller transitions, in combination with a difference in Coulomb energy shifts for ^{40}Ar and ^{40}Ti, can produce the differences on the scale of those observed between the ^{40}Ar charge-exchange and ^{40}Ti β-decay data. In combination with the difference in nuclear penetrability of the (p,n) and (^{3}He,t) probes, the different contributions from amplitudes associated with transitions in the pf and sd shells are likely also responsible for the observed discrepancy between the ratio of the cross sections for the low-lying 1^+ states in the ^{40}Ar(p,n) and ^{40}Ar(^{3}He,t) data.

Conclusions: On the basis of this study, it is recommended to use Gamow-Teller strengths extracted from the ^{40}Ar(p,n) data, not the ^{40}Ti β-decay data, for the calculation of neutrino capture rates. Further theoretical studies are required to achieve a consistent quantitative description for the energy differences between low-lying 1^+ states in ^{40}K and ^{40}Sc and the experimentally observed Gamow-Teller strengths.

DOI: 10.1103/PhysRevC.89.064313 PACS number(s): 21.60.Cs, 25.30.Pt, 25.40.Kv, 27.40.+z

*zegers@nscl.msu.edu
†Present address: Department of Nuclear Engineering and Health Physics, Idaho State University, Idaho 83208, USA.
‡Present address: Department of Physics and Astronomy, Rowan University, Glassboro, New Jersey 08028, USA.
§Present address: NIRS, Inage, Chiba 263-8555, Japan.
‖Present address: Los Alamos National Laboratory, Los Alamos, New Mexico 87545, USA.
¶Present address: Comisión Chilena de Energía Nuclear, Post Office Box 188-D, Santiago, Chile.
**Deceased.
††Department of Physics, Central Michigan University, Mount Pleasant, Michigan 48859, USA.
‡‡Present address: Institute for Work Design of North Rhine-Westphalia, Radiation Protection Services, 40225 Düsseldorf, Germany.
§§Present address: CYRIC, Tohoku University, Aramaki, Aoba, Sendai 980-8578, Japan.
‖‖Present address: RIKEN, Nishina Center, Wako, Saitama 351-0198, Japan.

I. INTRODUCTION

It has long been realized that liquid argon is a suitable medium for neutrino detection. Its properties have motivated the construction of a liquid argon time projection chamber [1] for the "Imaging Cosmic and Rare Underground Signal" (ICARUS) experiment [2] at the Laboratori Nazionali del Gran Sasso underground laboratory. With the completion of the detector system, a broad neutrino-physics program is under way [2,3], which includes the study of solar and supernova neutrinos in the energy range of $E_\nu \sim 5$–50 MeV. Recently, the ArgoNeuT collaboration presented first measurements of inclusive neutrino charged current differential cross sections on argon using a liquid argon time projection chamber [4], indicating the important usages of such a system.

The detection in liquid argon of neutrinos in this energy range relies on two reaction types: the elastic scattering of μ, τ and e neutrinos on electrons $[e^-(\nu_x,\nu_x)e^-]$ and the electron neutrino absorption via the $^{40}\mathrm{Ar}(\nu_e,e^-)^{40}\mathrm{K}^*$ reaction. Whereas the elastic scattering cross section can be calculated accurately [5], the estimation of the neutrino absorption rate is more complicated. The total rate has a Fermi and Gamow-Teller (GT) component. The Fermi transition strength $B(\mathrm{F})$, owing to the transition between the $^{40}\mathrm{Ar}(0^+)$ ground state and its isobaric analog state in ^{40}K, is governed by a model-independent sum rule [6] and carries little uncertainty. However, the determination of GT transition strengths $B(\mathrm{GT})$ [here defined such that for the decay of the free neutron $B(\mathrm{GT}) = 3$] is not as straightforward, owing to transitions to multiple 1^+ states in ^{40}K.

Two experimental methods have been used to determine the relevant GT transition strengths. In the first method, one uses GT strengths measured in the β decay of ^{40}Ti [7–9] and assumes isospin symmetry. If this assumption is valid, the measured transition strengths from ^{40}Ti to ^{40}Sc are equal to the analog transitions from ^{40}Ar to ^{40}K. The second method relies on the extraction of GT strengths through (p,n)-type charge-exchange reactions on ^{40}Ar that populate the 1^+ states in ^{40}K [8,10]. No assumptions on isospin symmetry are required, but the extraction of the GT strength relies on its proportionality (expressed through the so-called "unit cross section") to the charge-exchange cross section at vanishing linear momentum transfer ($q \approx 0$) [11]. It is known that the uncertainty in the proportionality can be sizable for transitions with small $B(\mathrm{GT})$ [11–13] mostly owing to interference between the central $\sigma\tau$ component (which mediates the $\Delta L = 0$, $\Delta S = 1$ GT transitions) and the noncentral tensor component (which mediates $\Delta L = 2$, $\Delta S = 1$ transitions) of the effective nucleon-nucleon interaction. Both contribute to the $\Delta J = 1$, $0^+ \rightarrow 1^+$ excitation in charge-exchange reactions. For transitions of significant GT strength, the uncertainties are usually small and a deviation of ∼20% for $B(\mathrm{GT}) \sim 0.3$ is among the highest reported [14]. However, as first reported in Ref. [8] and more recently investigated in detail in Ref. [10], a large discrepancy exists between the GT transition strengths derived from β^+ decay of ^{40}Ti and those extracted from $^{40}\mathrm{Ar}(p,n)$ charge-exchange data. The experimental data are shown in Figs. 1(a) and 1(b). Although at higher excitation energies the differences can partially be attributed to the limited resolution

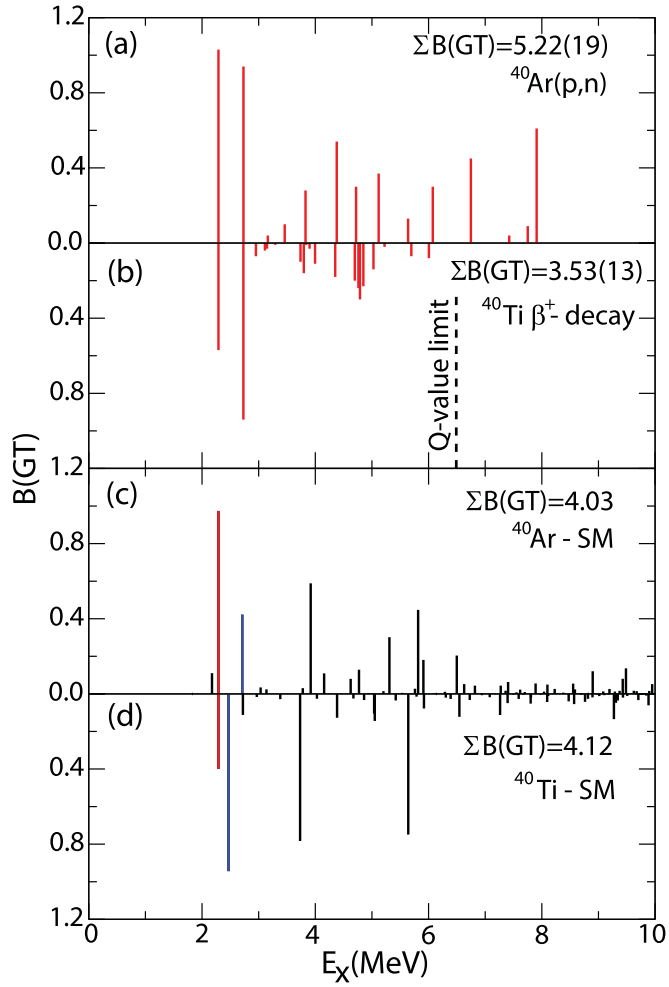

FIG. 1. (Color online) GT strength distributions in the $A = 40$, $T = 2$ isoquintet. (a) Extracted from $^{40}\mathrm{Ar}(p,n)$ [10]. (b) Extracted from β^+ decay of ^{40}Ti. The dashed line indicates the limit of the Q-value window available for β^+ decay. (c) Shell-model calculations for transitions from ^{40}Ar to ^{40}K. (d) Shell-model calculations for transitions from ^{40}Ti to ^{40}Sc.

of the (p,n) experiment so that several weaker transitions in the β^+ decay are not observed or merged together, for the strong transition to the first 1^+ state at 2290 keV, the discrepancy is unusually large (80%): A $B(\mathrm{GT})$ of 1.03(10) is reported from the $^{40}\mathrm{Ar}(p,n)$ experiment and 0.57(3) [10] from the β-decay experiment [9].[1] The $B(\mathrm{GT})$ values for the transition to the second 1^+ states at 2730 keV are identical: 0.94(9) in the case of β decay and 0.94(4) from the (p,n) measurement. Therefore, even in the unlikely case of the absolute normalization of the (p,n) data being wrong by a factor that would explain the deviations for the transition to the state at 2290 keV, a large discrepancy remains when considering the ratio

$$R = \frac{B(\mathrm{GT})_{2730\ \mathrm{keV}}}{B(\mathrm{GT})_{2290\ \mathrm{keV}}}. \quad (1)$$

[1] $B(\mathrm{GT})$ Values reported from β decay of ^{40}Ti for the states of relevance to this work are consistent between Refs. [7–9] and we used those from [9].

TABLE I. Experimental and shell-model B(GT) values and their ratios for the transitions to the 1^+ states at 2290 and 2730 keV.

E_x(^{40}K) (keV)	$B(\mathrm{GT})_{\mathrm{exp}}$			$B(\mathrm{GT})_{\mathrm{SM}}$[d]	
Ref. [15]	(p,n)[a]	$\beta(^{40}\mathrm{Ti})$[b]	$(^3\mathrm{He},t)$[c]	$^{40}\mathrm{Ar}\rightarrow{}^{40}\mathrm{K}$	$^{40}\mathrm{Ti}\rightarrow{}^{40}\mathrm{Sc}$
2289.87(1)	1.03(10)	0.57(3)	—	0.97	0.40
2730.37(2)	0.94(9)	0.94(4)	—	0.42	0.94
R	0.911(5)	1.65(11)	0.73(5)	0.43	2.35

[a]From Ref. [10].
[b]From Ref. [9] and using isospin symmetry.
[c]Only the relative strengths for the two states are known experimentally.
[d]The shell-model calculations have been multiplied by a factor 0.60 to account for quenching of the GT strength [16].

The B(GT) values and R derived from $^{40}\mathrm{Ar}(p,n)$ and β-decay of ^{40}Ti are listed in columns 2 and 3 of Table I.

As shown in Fig. 7 of Ref. [10], the discrepancy observed for the transition to the state at 2290 keV has a significant effect on the neutrino capture rates on ^{40}Ar. Usage of the $^{40}\mathrm{Ar}(p,n)$ values, rather than the $^{40}\mathrm{Ti}(\beta^+)$ values, results in a rate increase by a factor that ranges from 1.3 at $E_\nu = 30$ MeV to 1.8 at threshold ($E_\nu = 8$ MeV), assuming the threshold for the detection of the outgoing electron is 5 MeV.

In Ref. [17], a combination of three effective interactions was used to calculate the GT strength distribution: sdpf-m for the sd shell [18], GXPF1J for the pf shell [19–21], and the SDPF-VMU-LS interaction for the sd-pf cross-shell parts [22,23]. This calculation reproduced the overall strength distribution extracted from the $^{40}\mathrm{Ar}(p,n)$ reaction better than an earlier shell-model calculation of Ref. [24]. It also produced a value $R < 1$, consistent with the $^{40}\mathrm{Ar}(p,n)$ data, and hence in contrast to the results from the $\beta(^{40}\mathrm{Ti})$ data.

This work was aimed at improving our understanding of the discrepancy between the GT strengths extracted from the $\beta(^{40}\mathrm{Ti})$ data and from the $^{40}\mathrm{Ar}(p,n)$ data for the transitions to the final states at 2290 and 2730 keV. Under the assumption that the available data are of good quality, two possible reasons were investigated: (i) an underlying nuclear structure issue causes a large discrepancy between the two sets of data, (ii) the proportionality between GT transition strength and the cross section at $q = 0$ for the charge-exchange reaction is severely broken owing to a complicated reaction process. For studying (i), shell-model calculations were performed and results are described in Sec. II. For the investigation of (ii) detailed distorted-wave Born approximation (DWBA) calculations for the $^{40}\mathrm{Ar}(p,n)$ reaction to the two strongly excited 1^+ transitions are required. In addition, new high-resolution data for the $^{40}\mathrm{Ar}(^3\mathrm{He},t)$ reaction became available and were used to complement the reaction studies. A comparison of the extracted GT strengths from the two different charge-exchange probes has been shown to be a good tool to understand complications in the reaction mechanism; see, e.g., Refs. [14,25] for the cases of ^{58}Ni and ^{13}C, respectively. The reaction studies are discussed in Sec. III.

II. STRUCTURE STUDIES

The shell-model calculations were carried out in the sd-pf model space $(sd)^{20}(pf)^2$ for all $A = 40$ positive-parity states with $T = 1$ and 2. The starting point of the calculations was the WBMB Hamiltonian that was constructed in Ref. [26]. This Hamiltonian was also used by Ormand *et al.* [24] for calculating neutrino capture cross sections on ^{40}Ar and β decay of ^{40}Ti. This interaction conserves isospin; the calculated spectra of the mirror nuclei are identical and the calculated mirror B(GT) values are the same. The WBMB Hamiltonian was then updated by including the Coulomb interaction between protons. Also, the single-particle energies in WBMB were modified to reproduce the experimental binding-energy differences for ^{41}Ca-^{40}Ca (neutron pf), ^{41}Sc-^{40}Ca (proton pf), ^{40}Ca-^{39}Ca (neutron sd), and ^{40}Ca-^{39}K (proton sd). The resulting Hamiltonian is called WBMB-C.

The WBMB-C Hamiltonian mixes isospin; the calculated spectra of the mirror nuclei are different and the calculated B(GT) mirror values are not equal, as shown in Figs. 1(c) and 1(d) for the $^{40}\mathrm{Ar}\rightarrow{}^{40}\mathrm{K}$ and $^{40}\mathrm{Ti}\rightarrow{}^{40}\mathrm{Sc}$ channels, respectively. The differences in the GT strength distribution can be understood in terms of the dominant components of the wave functions:

$$^{40}\mathrm{Ar}\ \ [(\pi sd)^{-2}(J,T) = (0,1)] \times [(\nu pf)^2(J,T) = (0,1)],$$
$$^{40}\mathrm{Ti}\ \ [(\nu sd)^{-2}(J,T) = (0,1)] \times [(\pi pf)^2(J,T) = (0,1)].$$

For the $^{40}\mathrm{Ar}\rightarrow{}^{40}\mathrm{K}$ transition the GT operator acting on ^{40}Ar ground state can make two types of states in ^{40}K:

$$\text{(a)}\ [(\pi sd)^{-2}(J,T) = (0,1)] \times [(\nu pf)(\pi pf)(J,T) = (1,0)]$$

and

$$\text{(b)}\ [(\nu sd)^{-1}(\pi sd)^{-1}(J,T) = (1,0)] \times [(\nu pf)^2(J,T) = (0,1)].$$

For the $^{40}\mathrm{Ti}\rightarrow{}^{40}\mathrm{Sc}$ transition the GT operator acting on the ^{40}Ti ground state can make two types of states in ^{40}Sc:

$$\text{(a)}\ [(\nu sd)^{-2}(J,T) = (0,1)] \times [(\nu pf)^{-1}(\pi pf)^{-1}(J,T) = (1,0)]$$

and

$$\text{(b)}\ [(\nu sd)(\pi sd)(J,T) = (1,0)] \times [(\pi pf)^2(J,T) = (0,1)].$$

The total GT strength is an interference between components (a) and (b). The Coulomb interaction enters into the energy differences for (a)

$$E\{[(\pi sd)^{-2}(J,T) = (0,1)]\} - E\{[(\nu sd)^{-2}(J,T) = (0,1)]\}$$

and (b)

$$E\{[(\pi pf)^2(J,T) = (0,1)]\} - E\{[(\nu pf)^2(J,T) = (0,1)]\},$$

where E is the negative of the binding energy.

These are related to the experimental energy differences,

$$E(^{38}\mathrm{Ca}) - E(^{38}\mathrm{Ar}) = 14.22\ \mathrm{MeV}$$

and

$$E(^{42}\mathrm{Ti}) - E(^{42}\mathrm{Ca}) = 14.99\ \mathrm{MeV},$$

respectively. The WBMB-C Hamiltonian reproduces these differences rather well, 14.18 and 15.01 MeV, respectively.

The consequence is that the *sd* part of the GT (b) amplitude is shifted up relative to the *pf* part (a). The maximal shift would be about 0.8 MeV, but because there are other smaller components in these wave functions with a smaller Coulomb energy shift, the effective value is about 0.4 MeV. Owing to the interference between components (a) and (b), states that lie closer than about 0.4 MeV will have individual GT strengths that will be strongly influenced by this Coulomb shift, but the total strength (over an averaging interval about 1 MeV) will remain about the same.

From Figs. 1(c) and 1(d) it is clear that the transition strengths to the two low-lying states are very different for the two channels; the values are also listed in columns 5 and 6 of Table I. We note that the strength distribution for the ^{40}Ar $\rightarrow$ ^{40}K channel resembles the recent calculations of Ref. [17], in particular for the two low-lying transitions: In both cases, the ratio R as defined in Eq. (1) is much smaller than 1. For the calculated strengths in the ^{40}Ti $\rightarrow$ ^{40}Sc channel, R is clearly very different, and much larger than 1. It is, therefore, immediately clear that within a consistent shell-model calculation for the GT transition strengths in the ^{40}Ar $\rightarrow$ ^{40}K and ^{40}Ti $\rightarrow$ ^{40}Sc channels the ratio R can indeed be very different owing to the interference effects described above.

Even though the main features of the observed asymmetry between the ^{40}Ti $\rightarrow$ ^{40}Sc and the ^{40}Ar $\rightarrow$ ^{40}K channels are qualitatively described by the shell-model calculations, there exist notable differences. Experimentally, the summed GT strengths for the two strong low-lying transitions are rather different for the ^{40}Ti $\rightarrow$ ^{40}Sc (1.51 ± 0.05) and ^{40}Ar $\rightarrow$ ^{40}K (1.94 ± 0.16) channels, whereas in the shell-model calculations the values are nearly identical (1.34 and 1.39 for the ^{40}Ti $\rightarrow$ ^{40}Sc and ^{40}Ar $\rightarrow$ ^{40}K channels, respectively). In addition, the difference in excitation energy between the two levels is not well reproduced in the ^{40}Ti $\rightarrow$ ^{40}Sc channel, which could affect the mixing between different configurations. To achieve a better qualitative description of the data, significant further improvements to the shell-model Hamiltonian that go beyond the relatively simple corrections made here are required. Nevertheless, even though the shell-model calculations do not exactly reproduce the data, it is clear that one cannot simply rely on isospin symmetry and use the ^{40}Ti $\rightarrow$ ^{40}Sc channel for estimating strengths in the ^{40}Ar $\rightarrow$ ^{40}K channel.

III. REACTION MECHANISM

In the extraction of GT strengths from charge-exchange data, the ratio R can also be affected if the proportionality between strength and differential cross section is different for different transitions. This proportionality is expressed through the unit cross section $\hat{\sigma}$ defined as

$$\hat{\sigma} = \frac{(d\sigma/d\Omega)_{q=0}}{B(\mathrm{GT})}, \tag{2}$$

where $(d\sigma/d\Omega)_{q=0}$ is the differential cross section at vanishing linear momentum transfer. Similar to Eq. (1), we define

$$R_{\hat{\sigma}} = \frac{\hat{\sigma}_{2730\ \mathrm{keV}}}{\hat{\sigma}_{2290\ \mathrm{keV}}}. \tag{3}$$

If $R_{\hat{\sigma}} \neq 1$ it indicates that the relative strengths extracted from the charge-exchange data for the transitions to these states will have an error associated with the reaction mechanism. Because such an error would not be present in the extraction of the GT strengths from β-decay data, it would lead to a difference between the strengths extracted for the ^{40}Ar $\rightarrow$ ^{40}K and ^{40}Ti $\rightarrow$ ^{40}Sc channels.

We studied the ratio $R_{\hat{\sigma}}$ for the ^{40}Ar(p,n) reaction in DWBA by using the code DW81 [27]. The Love-Franey effective nucleon-nucleon (*NN*) interaction at 140 MeV [28,29] was employed and exchange effects were treated exactly. One-body transition densities (OBTDs) for the transitions from the ^{40}Ar ground state to the excited states at 2730 and 2290 keV in ^{40}K were taken from the above-described shell-model calculations with the WBMB-C Hamiltonian. Radial wave functions of the target and residual nuclei were calculated using a Woods-Saxon potential (with radius parameter $r_0 = 1.25$ fm and diffusiveness $a = 0.65$ fm [30]). Single-particle binding energies were determined using the Skyrme SK20 interaction [31]. Optical-model potential parameters for the proton (neutron) in the in (out)going channel were based on the global parametrization of Koning and Delaroche [32]. Because the extraction of GT strengths from ^{40}Ar(p,n) data in Ref. [10] relied on the empirically established energy-dependent ratio of the unit cross sections for GT and Fermi transitions [11], we calculated this ratio in the above framework as a cross-check. A ratio of 5.1 was found, which is consistent with the empirical value of 4.8 ± 0.3.

Three separate calculations were performed: a full DWBA calculation, a calculation in DWBA in which the tensor interaction of the effective *NN* interaction was switched off, and a calculation in plane-wave Born approximation (PWBA) in which the depth of the optical potentials were set to zero, and Coulomb forces were switched off as well. The latter calculation gives $R_{\hat{\sigma}} = 1$ and was carried out as a cross-check. The values for $R_{\hat{\sigma}}$ for the two sets of DWBA calculations are shown in Table II. In the DWBA calculation without the tensor component of the effective *NN* interaction, $R_{\hat{\sigma}}$ is slightly lower than unity, indicating differences between the transition densities for the excitations of the 1^+ states at 2730 and 2290 keV. When the tensor interaction is switched on, $R_{\hat{\sigma}}$ is slightly larger than unity, indicating minor interference effects between $\Delta L = 0$ and $\Delta L = 2$ amplitudes that are slightly different for the two $\Delta J = 1$ excitations. However, on the basis of these calculations, there is no indication that the differences between the GT strengths extracted from the ^{40}Ar(p,n) and β-decay of ^{40}Ti data are largely attributable to problems with assumptions made about the reaction mechanism of the (p,n) data.

To obtain further insight, an additional study was performed on the basis of recently acquired data for the ^{40}Ar(^{3}He,t) reaction at 140 A MeV. Details of the ^{40}Ar(^{3}He,t) experiment

TABLE II. Summary of the DWBA calculations for the (p,n) and (^{3}He,t) reactions on ^{40}Ar.

	$R_{\hat{\sigma}}$	
	DWBA	DWBA w/o tensor
^{40}Ar(p,n)	1.04	0.95
^{40}Ar(^{3}He,t)	0.72	0.79

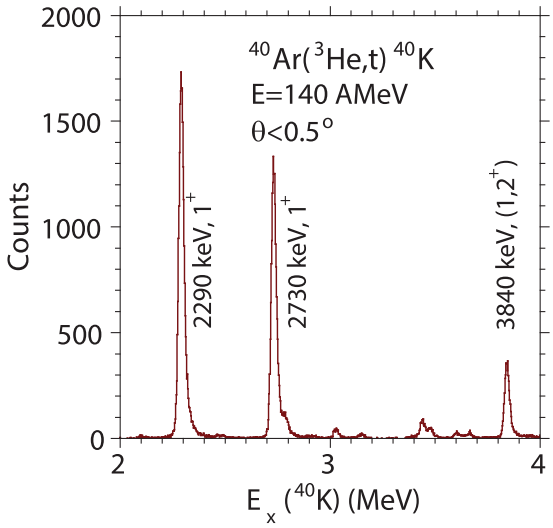

FIG. 2. (Color online) Excitation energy spectrum for the ^{40}Ar(^{3}He,t) reaction at 140 A MeV and at 0°, showing only the excitation energy range of relevance for the study of the strong transitions at 2730 and 2290 keV.

will be published in a forthcoming publication; here the focus is solely on the ratio of the transitions to the final 1^+ states in ^{40}K at 2290 and 2730 keV at scattering angles near zero degrees. A comprehensive overview of high-resolution (^{3}He,t) experiments can be found in Ref. [33].

A beam of ^{3}He particle was impinged on a ^{40}Ar gas target [34] contained by Aramid foils, which was placed at the target position of the Grand Raiden Spectrometer [35] at RCNP. Tritons were detected in the focal plane of the spectrometer and from the measurement of the position and angle in the focal plane, the excitation energy in ^{40}K and the scattering angle were determined. An excitation energy resolution of 30 keV was achieved by applying dispersion matching and focus matching techniques [33,36,37]. An angular resolution of ∼5 mrad was achieved by applying the angular matching technique [36] and the overfocus mode of the spectrometer [38]. The excitation-energy spectrum containing the state at 2290 and 2730 keV is shown in Fig. 2. The relative cross section to the two 1^+ states could easily be extracted, and owing to the excellent excitation-energy resolution achieved, the minor contribution from a contaminant state observed on the shoulder of the 2730-keV state (probably from the excitation of the 3^+ state at 2787 keV [15]) could be separated and subtracted by modeling the response of a single excitation by the shape of the transition to the 2290-keV state.

Under the assumption that the unit cross section for both transitions is the same, the extracted ratio of these cross sections is equal to the ratio R of the GT strengths for the two transitions [see Eq. (1)]. Because the excitation energies of the two states are very close, we note that the effects of the slight difference in linear momentum transfer for the extraction of the GT strengths is negligible. A value of $R = 0.73(5)$ was found (see also Table I), which is even smaller than the value of $R = 0.911(5)$ reported for the ^{40}Ar(p,n) reaction. The uncertainty in the extracted value of R from the (^{3}He,t) includes a systematic component owing to the modeling of the response function and the subtraction of the contaminant peak. However, the ^{40}Ar(^{3}He,t) data confirm the large discrepancy between the GT strengths extracted for the two low-lying states from the ^{40}Ar(p,n) data and the ^{40}Ti β-decay data.

In an attempt to understand the difference in R between the ^{40}Ar(p,n) and ^{40}Ar(^{3}He,t) data, DWBA calculations for the latter reaction were also performed. The code package FOLD [39] was used in the calculations. The structure input (OBTDs) was identical to that used for the ^{40}Ar(p,n) reaction. For the ^{3}H and ^{3}He particles, radial densities obtained from variational Monte Carlo calculations [40] were used in the calculation of the form factor, which was done by double folding the Love-Franey effective NN interaction [28,29] over the transition densities of the ^{40}Ar-^{40}K and ^{3}He-t systems. A short-range approximation following Ref. [28] for the effects of the antisymmetrization of the dinuclear system (the so-called "knock-on" exchange terms) was used. The optical potential parameters for the incoming channel were deduced from interpolating parameters obtained from the analysis of ^{3}He elastic scattering data on a wide variety of nuclei [41–43]. Following Ref. [44], the depths of the triton optical potentials for the outgoing channel were scaled to 85% of the ones for the ^{3}He particles.

The ratio $R_{\hat{\sigma}}$ of Eq. (3) was determined for the ^{40}Ar(^{3}He,t) reaction to the 1^+ states in ^{40}K at 2290 and 2730 keV and compared with the results for the ^{40}Ar(p,n) reaction. In PWBA, $R_{\hat{\sigma}} = 1$, as expected, but in DWBA (regardless of whether the tensor component of the NN interaction was switched on or off), $R_{\hat{\sigma}} < 1$ (see Table II), indicating that the unit cross sections for the two transitions are significantly different (by 20%–30%). Consequently, on the basis of these calculations, one expects that the differential cross section for the transition to the state at 2290 keV in the ^{40}Ar(^{3}He,t) data is enhanced (or the cross section to the 2730-keV state reduced) compared to the results of the ^{40}Ar(p,n) experiment, which is what is observed: The value of R in Table I is 25% larger in the ^{40}Ar(p,n) data than in the ^{40}Ar(^{3}He,t) data. More explicitly, if the values of R in Table I are adjusted for the calculated values of $R_{\hat{\sigma}}$ in Table II, $R_{(p,n)} = 0.87(5)$ and $R_{(^{3}\mathrm{He},t)} = 1.01(5)$. Although not quite consistent, these values of R are significantly closer to each other than without the correction.

We also note that the value of $R_{\hat{\sigma}}$ for the ^{40}Ar(^{3}He,t) reaction increases when the tensor interaction is excluded from the DWBA calculation, which is in contrast to the result for the ^{40}Ar(p,n) reaction. (A similar effect, namely that the interference between $\Delta L = 0$ and $\Delta L = 2$ amplitudes mediated by the tensor interaction is opposite in sign for the (p,n) and (^{3}He,t) reactions, was observed for the case of low-lying transitions in the case of ^{58}Ni [14].) Although the effects of the tensor interaction are smaller than the overall difference in $R_{\hat{\sigma}}$ for the two probes, they enhance the discrepancy.

The reason for the unusually high difference in unit cross sections for the two GT transitions from ^{40}Ar in the (^{3}He,t) reaction becomes clear when the radial transition density for each of these transitions is plotted (multiplied by r^2), as is done in Fig. 3. The transition density for the transition to the 1^+ state at 2290 keV (which, according to the shell-model calculations, is dominated by the $0f_{7/2}$-$0f_{7/2}^{-1}$ particle-hole transition) peaks at larger r and extends further than the

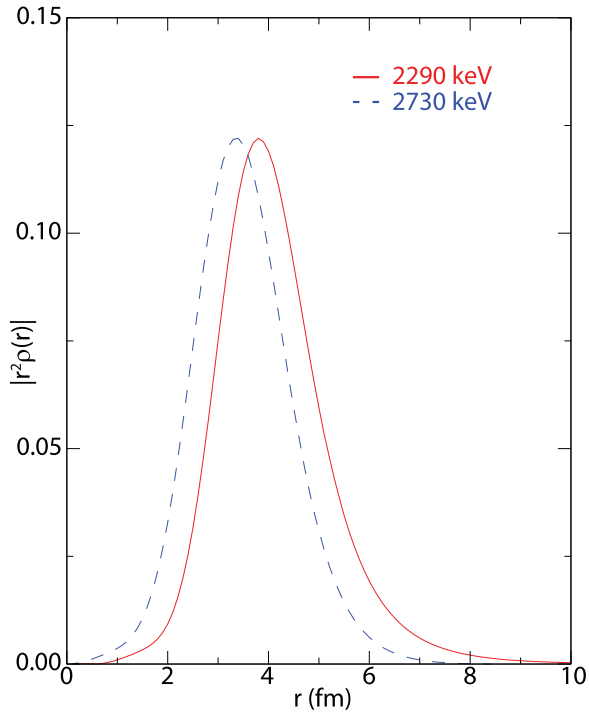

FIG. 3. (Color online) Radial transition densities (multiplied by r^2) for the transitions from ^{40}Ar to the 1^+ states at 2290 and 2730 keV. The vertical scales have been arbitrarily adjusted so that the peak values of the curves are equal.

transition density to the 1^+ state at 2730 keV (which is dominated by the $0d_{3/2}$-$0d_{3/2}^{-1}$ particle-hole transition). The (^{3}He,t) reaction probes the nuclear surface and is thus much more sensitive to differences between the shapes of transition densities than the (p,n) reaction, which probes further into the nuclear interior. We conclude that the difference between the values of R for the ^{40}Ar(p,n) and ^{40}Ar(^{3}He,t) reactions is, therefore, predominantly attributable to the difference in sensitivity to the shapes of the transition densities, with an additional but smaller enhancement owing to the effects of the tensor interaction. The observed discrepancy between the ^{40}Ar(p,n) and the ^{40}Ar(^{3}He,t) reactions for the strong transitions to the low-lying 1^+ states in ^{40}K is extremely rare, as extracted GT strengths from the two probes usually match well.

IV. CONCLUSIONS

The unusually large discrepancy between GT transition strengths extracted from the ^{40}Ar(p,n) reaction for the excitations of 1^+ states at 2290 and 2730 keV in ^{40}K and the GT strengths obtained for the analog transitions in the β decay of ^{40}Ti has been investigated on the basis of shell-model calculations in the sd-pf model space and studies of the reaction mechanism in DWBA for the ^{40}Ar(p,n) reaction. In addition, by comparison with newly obtained data for the ^{40}Ar(^{3}He,t) reaction, further insight in the reaction and structure aspects of the relevant transitions was obtained.

Although the theoretical calculations still have deficiencies, they provide insight in the underlying mechanisms responsible for the discrepancies between the GT strengths extracted from the analog channels in the charge-exchange and β-decay data. These mechanisms are predominantly related to interference effects between sd and pf contributions to the GT transitions. Although the transition to the 1^+ state at 2290 keV is dominated by pf-shell amplitudes and the transition to the state at 2730 keV is dominated by sd-shell amplitudes, interference effects between these amplitudes, which are sensitive to Coulomb shifts, cause large difference between the analog transitions. The comparison between the ^{40}Ar(p,n) and ^{40}Ar(^{3}He,t) data and associated studies of the reaction mechanisms confirm the difference in the nature of the GT transitions to the low-lying 1^+ states. Because the transition density associated with the excitation of the low-lying 1^+ state (dominated by pf-shell amplitudes) extends further than for the high-lying 1^+ state (dominated by sd-shell amplitudes), and the (^{3}He,t) reaction probes the nuclear surface whereas the (p,n) reaction probes deeper into the interior, a difference between the ratios of the cross sections for the two low-lying states in charge-exchange data sets was observed.

Although further development of the theoretical models is required to achieve better quantitative correspondence between the data and the theory, the present results give clear direction regarding a lingering ambiguity about the GT response of ^{40}Ar, which is important for the analysis and development of neutrino detectors based on liquid argon. For the purpose of these studies, it is recommended to use the GT transition strength extracted from the ^{40}Ar(p,n) data, which have limited uncertainties (less than 10%) associated with tensor component of the NN interaction and differences between the transition densities for the two low-lying GT transitions.

ACKNOWLEDGMENTS

The authors would like to thank the staff at the Research Center for Nuclear Physics (RCNP) in Osaka for their efforts and support during RCNP experiment E307. This work was supported by the U.S. NSF [Grants No. PHY-1102511, No. PHY-0822648 (JINA), and No. PHY-1068217], Grant No. TUBITAK-109T373, the Hungarian OTKA Foundation (Grant No. K106035), and MEXT, Japan (Program No. 18540270 and 22540310).

[1] C. Rubbia, Report No. CERN-EP/77-08, 1977.
[2] S. Amerio *et al.*, Nucl. Instrum. Methods A **527**, 329 (2004); see also http://icarus.lngs.infn.it/.
[3] F. Arneodo *et al.*, Reports No. LNGS-P28/2001, No. LNGS-EXP 13/89 add. 1/01, and No. ICARUS-TM/2001-03 (2001); http://icarus.lngs.infn.it/serwer/proposals/t600physup.pdf.
[4] C. Anderson *et al.*, Phys. Rev. Lett. **108**, 161802 (2012).
[5] J. N. Bahcall, M. B. Ceolin, D. B. Cline, and C. Rubbia, Phys. Lett. B **178**, 324 (1986).
[6] K. Ikeda, S. Fujii, and J. I. Fujita, Phys. Lett. **3**, 271 (1963).
[7] W. Trinder *et al.*, Phys. Lett. B **415**, 211 (1997).
[8] W. Liu *et al.*, Phys. Rev. C **58**, 2677 (1998).

[9] M. Bhattacharya *et al.*, Phys. Rev. C **58**, 3677 (1998).
[10] M. Bhattacharya, C. D. Goodman, and A. García, Phys. Rev. C **80**, 055501 (2009).
[11] T. D. Taddeucci *et al.*, Nucl. Phys. A **469**, 125 (1987).
[12] R. G. T. Zegers *et al.*, Phys. Rev. C **74**, 024309 (2006).
[13] G. W. Hitt *et al.*, Phys. Rev. C **80**, 014313 (2009).
[14] A. L. Cole *et al.*, Phys. Rev. C **74**, 034333 (2006).
[15] J. A. Cameron and B. Singh, Nucl. Data Sheets **102**, 293 (2004).
[16] B. H. Wildenthal, M. S. Curtin, and B. A. Brown, Phys. Rev. C **28**, 1343 (1983).
[17] T. Suzuki and M. Honma, Phys. Rev. C **87**, 014607 (2013).
[18] Y. Utsuno, T. Otsuka, T. Mizusaki, and M. Honma, Phys. Rev. C **60**, 054315 (1999).
[19] M. Honma, T. Otsuka, T. Mizusaki, M. Hjorth-Jensen, and B. A. Brown, J. Phys. Conf. Ser. **20**, 7 (2005).
[20] M. Honma, T. Otsuka, B. A. Brown, and T. Mizusaki, Phys. Rev. C **65**, 061301(R) (2002).
[21] M. Honma, T. Otsuka, B. A. Brown, and T. Mizusaki, Phys. Rev. C **69**, 034335 (2004).
[22] T. Otsuka, T. Suzuki, R. Fujimoto, H. Grawe, and Y. Akaishi, Phys. Rev. Lett. **95**, 232502 (2005).
[23] T. Otsuka, T. Suzuki, M. Honma, Y. Utsuno, N. Tsunoda, K. Tsukiyama, and M. Hjorth-Jensen, Phys. Rev. Lett. **104**, 012501 (2010).
[24] W. E. Ormand, P. Pizzochero, P. F. Bortignon, and R. A. Broglia, Phys. Lett. B **345**, 343 (1995).
[25] R. G. T. Zegers *et al.*, Phys. Rev. C **77**, 024307 (2008).
[26] E. K. Warburton, J. A. Becker, and B. A. Brown, Phys. Rev. C **41**, 1147 (1990).
[27] R. Schaeffer and J. Raynal, program DWBA70 (unpublished); J. R. Comfort, extended version DW81 (unpublished).
[28] W. G. Love and M. A. Franey, Phys. Rev. C **24**, 1073 (1981).
[29] M. A. Franey and W. G. Love, Phys. Rev. C **31**, 488 (1985).
[30] A. Bohr and B. Mottelson, *Nuclear Structure* (W. A. Benjamin, New York, 1969), Vol. I.
[31] B. A. Brown, Phys. Rev. C **58**, 220 (1998).
[32] A. J. Koning and J. P. Delaroche, Nucl. Phys. A **713**, 231 (2003).
[33] Y. Fujita, B. Rubio, and W. Gelletly, Prog. Part. Nucl. Phys. **66**, 549 (2011).
[34] H. Matsubara, A. Tamii, Y. Shimizu, K. Suda, Y. Tameshige, and J. Zenihiro, Nucl. Instrum. Methods Phys. Res. A **678**, 122 (2012).
[35] M. Fujiwara *et al.*, Nucl. Instrum. Methods Phys. Res. A **422**, 484 (1999).
[36] Y. Fujita *et al.*, Nucl. Instrum. Methods Phys. Res. B **126**, 274 (1997).
[37] H. Fujita *et al.*, Nucl. Instrum. Methods Phys. Res. A **484**, 17 (2002).
[38] H. Fujita *et al.*, Nucl. Instrum. Methods Phys. Res. A **469**, 55 (2001).
[39] J. Cook and J. Carr (1988), computer program FOLD, Florida State University (unpublished), based on F. Petrovich and D. Stanley, Nucl. Phys. A **275**, 487 (1977), modified as described in J. Cook, K. W. Kemper, P. V. Drumm, L. K. Fifield, M. A. C. Hotchkis, T. R. Ophel, and C. L. Woods, Phys. Rev. C **30**, 1538 (1984) and R. G. T. Zegers, S. Fracasso and G. Colò (2006) (unpublished).
[40] S. C. Pieper and R. B. Wiringa, Annu. Rev. Nucl. Part. Sci. **51**, 53 (2001); R. B. Wiringa (private communication).
[41] T. Yamagata *et al.*, Nucl. Phys. A **589**, 425 (1995); T. Yamagata and H. Akimune (private communication).
[42] J. Kamiya *et al.*, Phys. Rev. C **67**, 064612 (2003).
[43] R. G. T. Zegers *et al.*, Phys. Rev. Lett. **99**, 202501 (2007).
[44] S. Y. van der Werf, S. Brandenburg, P. Grasdijk, W. A. Sterrenburg, M. N. Harakeh, M. B. Greenfield, B. A. Brown, and M. Fujiwara, Nucl. Phys. A **496**, 305 (1989).